Desalination and Water Treatment
www.deswater.com

doi:10.5004/dwt.2018.22937

131 (2018) 1–8
November

Heat and mass transfer in sweeping gas membrane distillation

Nizar Loussif[a,b,*], Jamel Orfi[c]

[a]*Unité de Recherche Matériaux, Energie et Energies Renouvelables, Faculté des Sciences Gafsa, Université de Gafsa, Gafsa, Tunisia, Tel. 0021652772609, email: loussif_nizare@yahoo.fr (N. Loussif)*
[b]*École Nationale d›Ingénieur de Monastir, Université de Monastir, Monastir, Tunisia*
[c]*Mechanical Engineering Department, King Saud University, Riyadh, Saudi Arabia, Tel. 00966114679798, email: orfij@ksu.edu.sa (J. Orfi)*

Received 21 September 2017; Accepted 12 August 2018

ABSTRACT

Membrane distillation (MD) has been widely investigated the last two decades as a novel and promising technique for desalination. Four main configurations are commonly used and developed. Sweeping gas membrane distillation (SGMD) which is not enough investigated in the literature, consists of a hot saline solution and a binary gas flow (generally dry air and water vapor) separated by a hydrophobic membrane allowing just water vapor to pass. In this work, a numerical analysis is conducted to investigate the details of the heat and mass transfer in the channel where the sweeping gas flows. The physical model considers also the transport phenomena in the feed solution and the hydrophobic membrane. The axisymmetric flow field is modeled using the two dimensional steady-state partial differential equations expressing conservation of mass (overall and species), energy and momentum using constant fluid properties. Viscous dissipation, thermal radiation and Soret and Dufour effects are neglected. Appropriate boundary conditions are applied. Results are expressed in terms of velocity and temperature profiles as well as heat transfer coefficients. Pure water production and performance of the overall process are also investigated. The results show in particular that pure water production and thermal efficiency are very sensitive to inlet temperatures and inlet velocities of both flows (saline solution and sweeping air). For instance, increasing the sweeping air inlet velocity tends to enhance the gas heat transfer mechanism and to reduce that of the saline solution.

Keywords: Membrane distillation; Sweeping gas; Convection; Heat and mass transfer

1. Introduction

Membrane distillation (MD) is a membrane separation process which has been widely investigated the last two decades as a novel and promising technique for desalination. This is due mainly to its potential in desalination and numerous other separation applications as well as to its various advantages including the low levels of operating temperature and pressure in comparison with the usual membrane processes, its high rejection rates and its capability to treat high concentration saline waters.

The driving force in MD process is the difference in vapor pressure of water caused by an existing temperature difference across the membrane. The trans-membrane vapor pressure difference can be generated with several possibilities leading to four main configurations namely direct contact membrane distillation (DCMD), air gap membrane distillation (AGMD), vacuum membrane distillation (VMD) and sweeping gas membrane distillation (SGMD).

Many theoretical and experimental studies have been conducted to investigate the MD performance, particularly for DCMD, AGMD and VMD configurations, while SGMD configuration has received less attention. This may be attributed to the condensation process that takes place in an external condenser and its lower pure water production in comparison with AGMD and DCMD configurations operating under the same conditions [1,2]. SGMD can be used in various applications including desalination and pure water production from brackish waters, concentration of non-volatile acids, separation of azeotropic aqueous mixtures such

*Corresponding author.

1944-3994 / 1944-3986 © 2018 Desalination Publications. All rights reserved.

as alcohol/water mixtures and crystallization [3,4]. Important details and useful information on the advantages and characteristics of this MD configuration can be found in [5].

Experimental and theoretical investigations have been performed to investigate the SGMD performance in particular the permeate flux and the thermal efficiency for isopropanol water separation [6], wastewater containing ammonia [7], desalination [8,9], ethanol water separation [10] and sucrose aqueous solutions [11]. Karanikola et al. [12] investigated the effect of membrane characteristics and architecture and operational variables using a bench-scale, sweeping gas, flat-sheet Membrane Distillation (MD) unit. Results of simulations based on coupled mass and energy balances and on experimentally calibrated theoretical model have been presented.

Among the previous studies on SGMD, just few have been concerned with refined numerical analysis of the flows and the associated transport phenomena. The remaining studies are based on 1D and lumped simplified models using empirical heat and mass transfer correlations [3,5–8,11–19]. Charfi et al. [19] presented detailed numerical results on the flow with heat and mass transfer patterns in the fluid zones as well as in the membrane region using appropriate equations for micro-porous medium. Huang et al. [20] investigated the conjugate heat and mass transfer in a hollow fiber membrane tube bank with an in-line arrangement of a sweeping gas membrane distillation. A numerical model for various domains (tube side, membrane side, and shell side) has been developed and results expressing the friction factors, local and mean Nusselt and Sherwood numbers have been obtained. Besides, an experimental set up for validation purposes has been developed and used.

This work aims at contributing to understand the flow and transfer mechanisms and propose heat and mass transfer results by conducting a numerical simulation of a SGMD configuration. The effects of the SGMD operating conditions such as inlet temperatures and velocities will be presented and discussed. The developed code is validated with available experimental data from the literature.

2. Mathematical model

2.1. Process description

The present study deals with a numerical simulation of flows in a sweeping gas membrane distillation unit. Fig. 1 illustrates a descriptive diagram of the physical model considered. The 2D Cartesian coordinates are used. Hot saline solution flows inside a channel. The wall of this channel consists of a micro porous hydrophobic membrane through which only water vapor can diffuse and the liquid water is retained. Vapor is recovered through a sweeping air circulation and condensed elsewhere. The temperature difference between the inner and the outer membrane sides creates a partial pressure gradient forcing the vapor to diffuse through the membrane. The computation domain includes the flows and heat and mass transfers in the hot saline water and the sweeping gas. The efficiency of this process depends on the effectiveness of several physical phenomena including the vapor generation by evaporation and its transport through the membrane as well as its condensation.

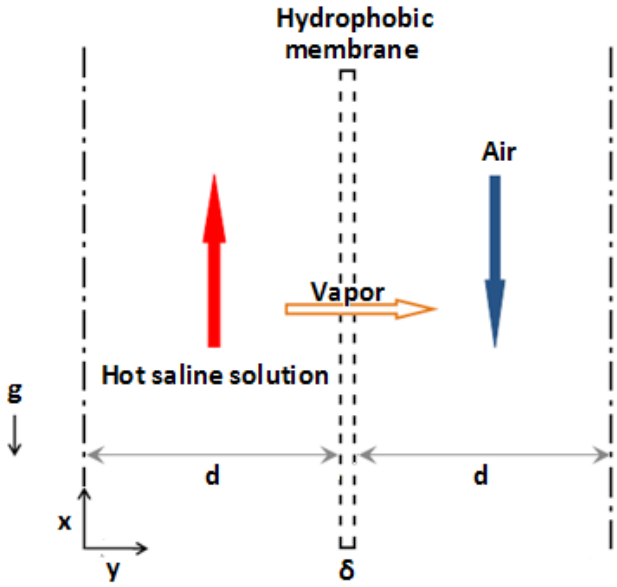

Fig. 1. Geometry and coordinate system of flow domain.

2.2. Governing equations

The partial differential equations governing the flow, heat and mass transfer within the hot feed saline water and the sweeping air are those of conservation of mass, momentum energy and species in x and y directions.

These equations are normalized using the following dimensionless variables (the suffixes s and a represent respectively the hot saline solution and the sweeping air).

$$\bar{x}=\frac{x}{d},\ \bar{y}=\frac{y}{d},\ \bar{U}=\frac{U}{U_s},\ \bar{V}=\frac{V}{U_s},\ \bar{P}=\frac{P}{\rho_s U_s^2},\ \bar{T}=\frac{T-T_a}{T_S-T_a},\ \bar{C}=\frac{C}{C_S} \quad (1)$$

$$\bar{x}=\frac{x}{d},\ \bar{y}=\frac{y}{d},\ \bar{U}=\frac{U}{U_a},\ \bar{V}=\frac{V}{U_a},\ \bar{P}=\frac{P}{\rho_a U_a^2},\ \bar{T}=\frac{T-T_a}{T_S-T_a} \quad (2)$$

U_s, T_s and C_s are respectively the inlet velocity, inlet temperature and inlet concentration of the saline solution. On the other side, U_a and T_a are respectively the inlet velocity and the inlet temperature of the sweeping air.

Therefore and after non dimensioning the governing equations and the boundary conditions, we obtain in the hot domain:

$$\frac{\partial\bar{U}}{\partial\bar{x}}+\frac{\partial\bar{V}}{\partial\bar{y}}=0 \quad (3)$$

$$\bar{U}\frac{\partial\bar{U}}{\partial\bar{x}}+\bar{V}\frac{\partial\bar{U}}{\partial\bar{y}}=-\frac{\partial\bar{P}}{\partial\bar{x}}+\frac{1}{\mathrm{Re}_S}\left(\frac{\partial^2\bar{U}}{\partial\bar{x}^2}+\frac{\partial^2\bar{U}}{\partial\bar{y}^2}\right) \quad (4)$$

$$\bar{U}\frac{\partial\bar{V}}{\partial\bar{x}}+\bar{V}\frac{\partial\bar{V}}{\partial\bar{y}}=-\frac{\partial\bar{P}}{\partial\bar{x}}+\frac{1}{\mathrm{Re}_S}\left(\frac{\partial^2\bar{V}}{\partial\bar{x}^2}+\frac{\partial^2\bar{V}}{\partial\bar{y}^2}\right) \quad (5)$$

$$\bar{U}\frac{\partial\bar{T}}{\partial\bar{x}}+\bar{V}\frac{\partial\bar{T}}{\partial\bar{y}}=\frac{1}{\mathrm{Re}_S\,\mathrm{Pr}_S}\left(\frac{\partial^2\bar{T}}{\partial\bar{x}^2}+\frac{\partial^2\bar{T}}{\partial\bar{y}^2}\right) \quad (6)$$

$$\overline{U}\frac{\partial\overline{C}}{\partial\overline{x}}+\overline{V}\frac{\partial\overline{C}}{\partial\overline{y}}=\frac{1}{\mathrm{Re}_S Sc_S}\left(\frac{\partial^2\overline{C}}{\partial\overline{x}^2}+\frac{\partial^2\overline{C}}{\partial\overline{y}^2}\right) \tag{7}$$

where the Reynolds, Prandlt and Schmidt of the hot saline solution are:

$$\mathrm{Re}_S=\frac{\rho_S U_S d}{\mu_S},\mathrm{Pr}_S=\frac{\mu_S Cp_S}{k_S},Sc_S=\frac{\upsilon_S}{D_S} \tag{8}$$

The boundary conditions in dimensionless form are:

- Inlet of the saline solution ($x = 0$)

$$\overline{U}=1,\overline{V}=0,\overline{T}=1,\overline{C}=1 \tag{9}$$

- Symmetry conditions ($y = 0$)

$$\frac{\partial\overline{U}}{\partial\overline{y}}=0,\frac{\partial\overline{T}}{\partial\overline{y}}=0,\frac{\partial\overline{C}}{\partial\overline{y}}=0,\overline{V}=0 \tag{10}$$

- Outlet of the saline solution ($x = L$)

$$\frac{\partial\overline{U}}{\partial\overline{x}}=0,\frac{\partial\overline{V}}{\partial\overline{x}}=0,\frac{\partial\overline{T}}{\partial\overline{x}}=0,\frac{\partial\overline{C}}{\partial\overline{x}}=0 \tag{11}$$

- Feed saline solution - membrane interface ($y = d$)

$$\overline{U}=0 \tag{12}$$

$$\overline{V}=\frac{J_v}{U_S\rho_S},\frac{\partial\overline{T}}{\partial\overline{y}}=\frac{d\left(Q_c+Q_L\right)}{k_S\left(T_a-T_S\right)},\frac{\partial\overline{C}}{\partial\overline{y}}=\frac{J_v d}{\rho_S D_S C_S} \tag{13}$$

where $Q_L = J_v h_{fg}$ represents the latent heat flux and Q_c the conduction heat flux.

In the sweeping gas domain, we suppose that there is no solute (NaCl) in the permeate side (vapor free of salt). Besides, we assume also that the generated vapor mass flow rate through the membrane is too limited and small compared to the mass flow rate of weeping air. It does not alter the thermo-physical of the sweeping gas.

The gas side govering equations and their corresponding boundary conditions are:

$$\frac{\partial\overline{U}}{\partial\overline{x}}+\frac{\partial\overline{V}}{\partial\overline{y}}=0 \tag{14}$$

$$\overline{U}\frac{\partial\overline{U}}{\partial\overline{x}}+\overline{V}\frac{\partial\overline{U}}{\partial\overline{y}}=-\frac{\partial\overline{P}}{\partial\overline{x}}+\frac{1}{\mathrm{Re}_a}\left(\frac{\partial^2\overline{U}}{\partial\overline{x}^2}+\frac{\partial^2\overline{U}}{\partial\overline{y}^2}\right) \tag{15}$$

$$\overline{U}\frac{\partial\overline{V}}{\partial\overline{x}}+\overline{V}\frac{\partial\overline{V}}{\partial\overline{y}}=-\frac{\partial\overline{P}}{\partial\overline{x}}+\frac{1}{\mathrm{Re}_a}\left(\frac{\partial^2\overline{V}}{\partial\overline{x}^2}+\frac{\partial^2\overline{V}}{\partial\overline{y}^2}\right) \tag{16}$$

$$\overline{U}\frac{\partial\overline{T}}{\partial\overline{x}}+\overline{V}\frac{\partial\overline{T}}{\partial\overline{y}}=\frac{1}{\mathrm{Re}_a\,\mathrm{Pr}_a}\left(\frac{\partial^2\overline{T}}{\partial\overline{x}^2}+\frac{\partial^2\overline{T}}{\partial\overline{y}^2}\right) \tag{17}$$

where the Reynolds and Prandlt numbers of the sweeping gas are:

$$\mathrm{Re}_a=\frac{\rho_a U_a d}{\mu_a},\mathrm{Pr}_a=\frac{\mu_a Cp_a}{k_a} \tag{18}$$

The boundary conditions in dimensionless form are:

- Inlet of the sweeping air domain ($x = L$)

$$\overline{U}=1,\overline{V}=0,\overline{T}=0 \tag{19}$$

- Symmetry conditions

$$\frac{\partial\overline{U}}{\partial\overline{y}}=0,\frac{\partial\overline{T}}{\partial\overline{y}}=0,\overline{V}=0 \tag{20}$$

- Outlet of the cold solution ($x = 0$)

$$\frac{\partial\overline{U}}{\partial\overline{x}}=0,\frac{\partial\overline{V}}{\partial\overline{x}}=0,\frac{\partial\overline{T}}{\partial\overline{x}}=0 \tag{21}$$

- Sweeping gas-membrane interface ($y = d+\delta$)

$$\overline{U}=0 \tag{22}$$

$$\overline{V}=0 \tag{23}$$

$$\frac{\partial\overline{T}}{\partial\overline{y}}=\frac{d\left(Q_c+Q_L\right)}{k_S\left(T_a-T_S\right)} \tag{24}$$

Stephan's law is used to give the general mass flux form Alklaibi and Lior [21]:

$$J_v=K\Delta P_v \tag{25}$$

where J_v is the local vapor flux generated across the membrane, K the permeability of the membrane and ΔP_v the water vapor pressure difference between the membrane sides;

The vapor pressure P_v can be calculated using the Antoine's equation:

$$P_v=\exp\left(23.1964-\frac{3816.44}{T-46.13}\right) \tag{26}$$

The membrane permeability K is defined for the molecular diffusion as [2,22–24]:

$$K=\frac{\varepsilon D_{v/a}M_v P_T}{\chi\delta_m P_{a,moy}RT_{moy,m}} \tag{27}$$

The effect of salt's presence in the solution on the vapor pressure at the hot surface of the membrane side has been considered and the Raoult's Law is used. So that, the vapor pressure at the hot saline solution-membrane interface P_{hm} is expressed as:

$$P_{hm}=(1-C_M)P_v \tag{28}$$

where C_M is the mole fraction of NaCl and P_v is the vapor pressure calculated used Antoine's equation at the temperature of the hot saline-membrane interface.

On the other hand, the total pressure may be written as function of the water vapor pressure corresponding to the air side of the membrane and the humidity ratio, w [14,25]:

$$P=\frac{P_v(w+0.622)}{w} \tag{29}$$

The humidity ratio along the membrane module length may be related with the air flux, m_a, and with the humidity at the membrane module inlet, w_a [14,25]:

$$w = w_a + \frac{J_v A}{m_a} \tag{30}$$

where A represents the membrane area. In the present study w_a will be considered equal to zero. Thus, the inlet air is considered as completely dry.

The total heat involved in such a process can be divided in two parts: the latent heat and the sensible one. The latent one is associated with the evaporation of the liquid water at the hot membrane side. While, the total sensible heat transfer Q_{sens} is transferred from the hot surface of the membrane to the sweeping air by:

heat conduction across the membranes Q_c;

the mass transfer of the vapor, Q_v:

$$Q_{sens} = Qc + Qv = \frac{T_1 - T_2}{R_m} \tag{31}$$

where T_1 is the temperature at the hot side of the membrane, T_2 is the temperature at the cold side of the membrane and R_m is the thermal resistance of the membrane defined by:

$$R_m = \frac{R_{mc} R_v}{R_{mc} + R_v} \tag{32}$$

where the heat transfer resistance of the solid part of the membrane is:

$$R_{mc} = \frac{\delta}{k_m} = \frac{\delta}{\varepsilon k_a + (1-\varepsilon) k_{ma}} \tag{33}$$

k_a and k_{ma} are the thermal conductivity of the air, and the membrane material, respectively. The heat transfer resistance of the vapor flow through the membrane pores is:

$$R_v = \frac{1}{J_v C p_v} \tag{34}$$

The averaged permeate flux is defined as:

$$J = \frac{1}{L}\int_0^L J_v(x)dx \tag{35}$$

The averaged conduction heat flux is:

$$\overline{Q_C} = \frac{1}{L}\int_0^L Q_C(x)dx \tag{36}$$

The averaged total latent heat flux is:

$$\overline{Q_L} = \frac{1}{L}\int_0^L Q_L(x)dx \tag{37}$$

The total heat transfer is:

$$\overline{Q_T} = \frac{1}{L}\int_0^L Q_T(x)dx \tag{38}$$

Therefore, the process thermal efficiency can be defined as:

$$\eta = \frac{\overline{Q_L}}{\overline{Q_T}} \tag{39}$$

The local heat transfer coefficients, h_{xs} and h_{xa} respectively for the saline solution and the sweeping air are defined by making equal convective and conductive heat transfer at the hot saline-membrane interface and the membrane-air flow interface respectively so that:

$$h_{xs} = \left.\frac{-k_s}{T_0 - T_1}\frac{\partial T}{\partial y}\right|_{y=d} \tag{40}$$

$$h_{xa} = \left.\frac{-k_a}{T_2 - T_3}\frac{\partial T}{\partial y}\right|_{y=d+\delta} \tag{41}$$

where T_0 represent the temperature at the center of the hot channel, T_1 the temperature at the saline solution-membrane interface, T_2 the temperature at the membrane-sweeping gas interface and T_3 the temperature at the center of cold channel.

3. Numerical method and validation

The control volume method and the Simpler algorithm [26] were used for the solution. A grid-dependence analysis of the method of solution was performed as mentioned in Table 1. The values are practically independent of the chosen grid. We select the grid size of 1000, 40 (1000 nodes in the axial direction and 40 in the transversal one) for the simulations conducted in this work. The computed results were validated by comparison with experimental data of Khayet et al. [14] and Charfi et al. [19] and were found to be in very good agreement, as shown in Fig. 2. The results of the simplified theoretical model developed by Khayet et al. [14] are also presented to show the difference between their model and the one presented in this study. It is obvious that our model fits better the experimental data.

4. Results and discussion

For all calculations, the following general conditions were considered: d = 2 mm, L = 20 cm, U_a = 1.5 m/s, U_s = 0.1 m/s, C_s = 0.025, T_a = 20°C, χ = 1.5, ε = 0.7, T_s = 65°C, δ = 0.4 mm, k_{ma} = 0.2 W/mK.

Fig. 3 presents the variations of the SGMD permeate flux as a function of inlet temperatures (T_s and T_a refer for saline solution and sweeping air respectively) and parameterized with inlet velocities (U_s and U_a respectively for saline solution and sweeping air).

As expected, increasing inlet saline solution temperature or decreasing inlet sweeping air temperature induces the increase of pure water production; this increase is enhanced by boosting one of the inlet velocities. In fact, the increase of inlet flow causes improvement of the heat transfer and

Table 1
Influence of grid size on the permeate flux and the thermal efficiency

Nx, Ny	1000,40	1200,40	1000,50	1200,50
J [kg/m^{2h}]	11.7811	11.7881	11.7899	11.7837
η	0.8680	0.8612	0.8688	0.8607

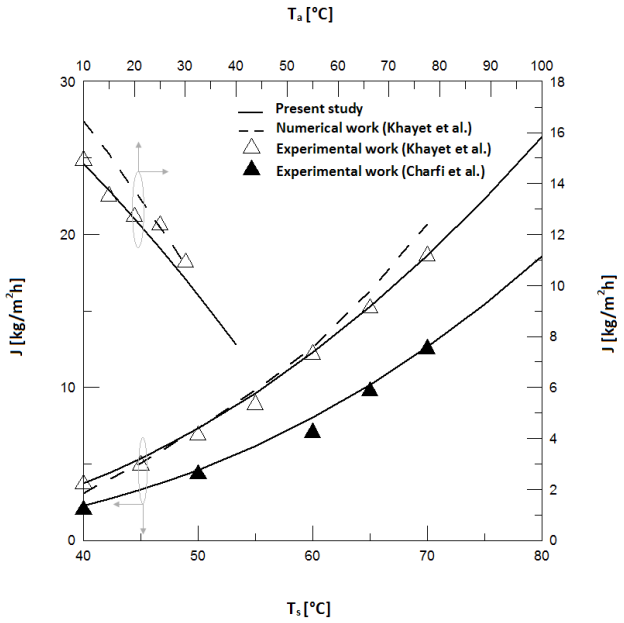

Fig. 2. Validation of the developed code with experimental data presented by Charfi et al. [19] and Khayet et al. [14].

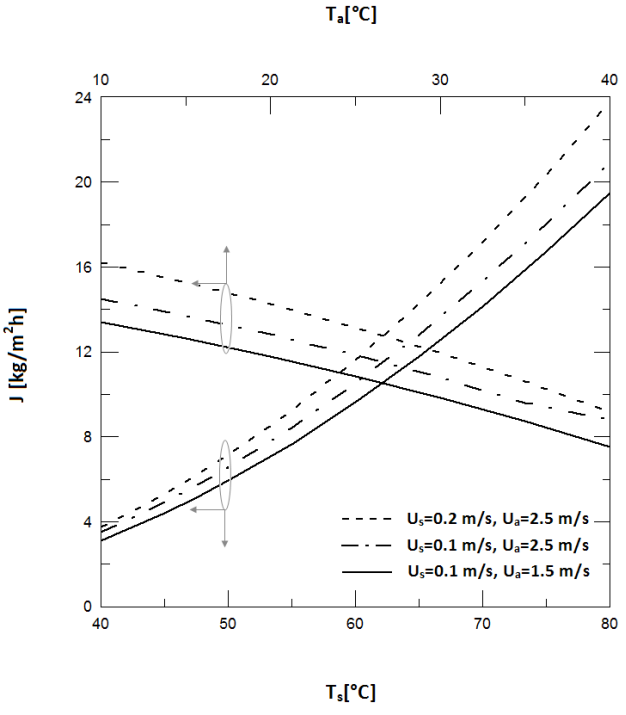

Fig. 3. Permeate flux evolution as a function of inlet temperatures and velocities.

makes the temperature at the membrane surface approaching the bulk temperature, and as a direct consequence, the driving force rises.

The variation of the thermal efficiency as a function of inlet temperatures for different inlet velocities is presented in Fig. 4. It is clear that, increasing inlet temperatures makes

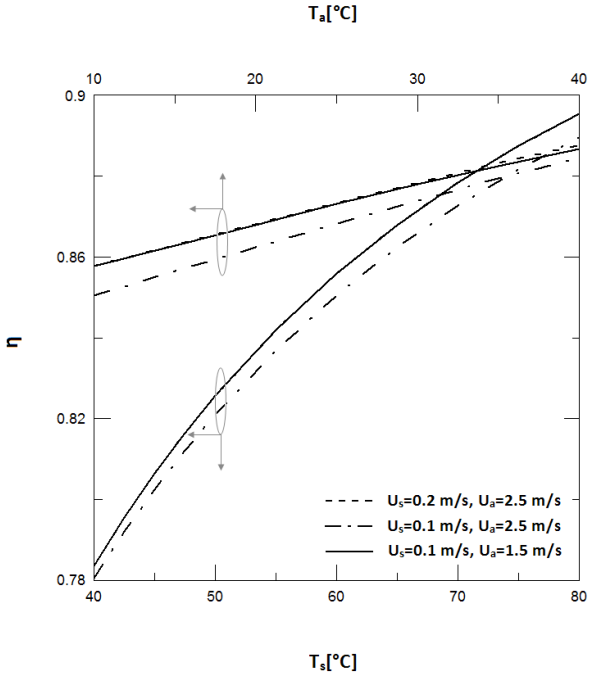

Fig. 4. Evolution of the process thermal efficiency as a function of inlet temperatures and velocities.

thermal efficiency higher. For a fixed saline solution inlet velocity (U_s = 0.1 m/s), increasing sweeping air velocity reduces slightly thermal efficiency while increasing saline solution inlet velocity for a fixed sweeping air velocity (U_a = 2.5 m/s) makes thermal efficiency rises again which presents opposite effects. While increasing inlet air and solution velocities results in an increasing in J, Q_c and Q_L. The decrease of η when rising U_a is attributed to the fact that the rate of increase of Q_L is lower than that of Q_C.

On the other side, the investigation of the heat and mass transfer behaviors is necessary to a better design and accurate evaluation of some output parameters used in the final design and construction of such desalination processes. Figs. 5 and 6 depict the axial variation along the channel of the heat transfer coefficients h_{xs} and h_{xa} respectively for the saline solution and the sweeping air as function of flow velocities. Two kinds of simulations have been done: varying the inlet hot saline solution velocity from 0.05 to 0.2 m/s (Fig. 5) and the sweeping air inlet velocity U_a from 0.5 to 2.5 m/s (Fig. 6).

Fig. 5 shows that both h_x decrease after entering the channel. For U_a = 1.5 m/s, varying U_s has no effect on the behavior of h_{xa} while h_{xs} decreases with U_s decrease. So we can conclude that the major heat transfer resistance of fluids occurs at the feed side.

In order to clarify and qualify the effect of the sweeping air inlet velocity on the heat transfer coefficients, Fig. 6 presents the variations of h_x with U_a when U_s is kept constant and equal to 0.1 m/s. Increasing sweeping air inlet velocity tends to increase the heat transfer of the gas and to decrease slightly the saline solution one.

Figs. 7 and 8 illustrate the effect of the membrane material thermal conductivity k_{ma} and membrane porosity ε on the permeate flux and the thermal efficiency. An increase of

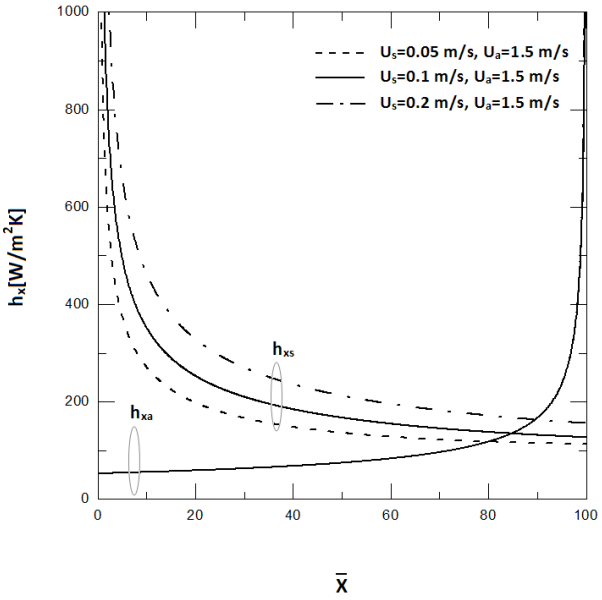

Fig. 5. Local heat transfer coefficients variations along the channel, h_{xs} and h_{xa} respectively for the saline solution and the sweeping air as a function of saline solution inlet velocity U_s.

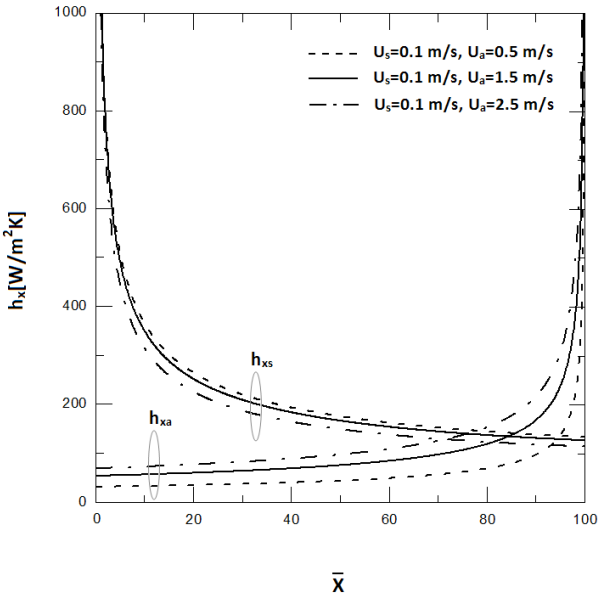

Fig. 6. Local heat transfer coefficients variations along the channel, h_{xs} and h_{xa} respectively for the saline solution and the sweeping air as a function of sweeping air inlet velocity U_a.

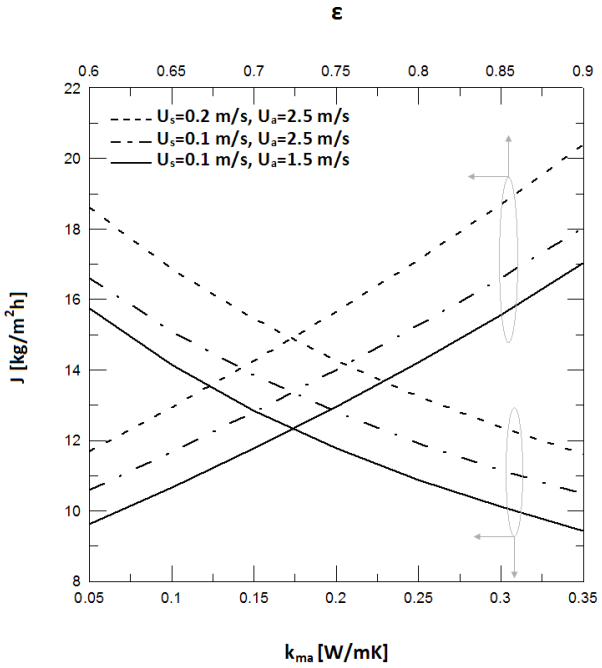

Fig. 7. Effect of membrane material thermal conductivity and porosity on the permeate flux.

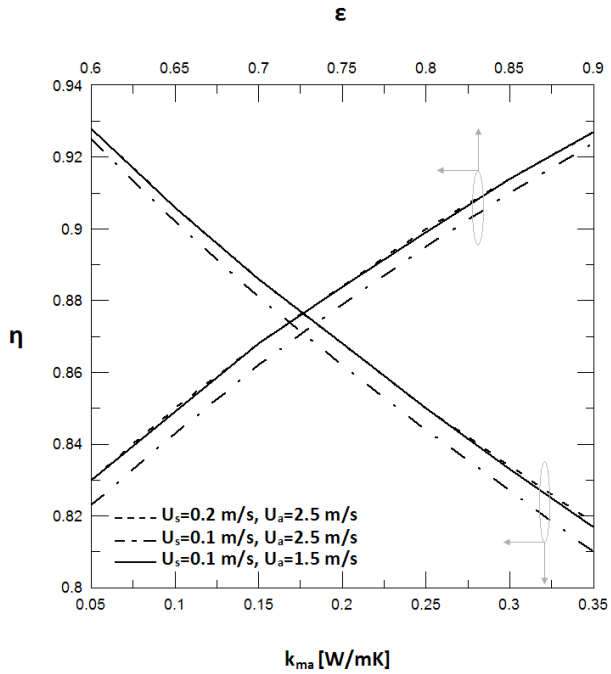

Fig. 8. Effect of membrane material thermal conductivity and porosity on the thermal efficiency.

water production by 66.84% occurred when k_{ma} decreases from 0.35 to 0.05 Wm^{-1} K^{-1}. Also, low values of k_{ma} enhance thermal efficiency. These increases result from the decrease of the effective thermal conductivity of the membrane which leaves much heat for water production. In the other side, increasing ε from 0.6 to 0.9 induces an increase of both J and η by 76.92 % and 11.68% respectively.

Fig. 9 shows the effect of the inlet concentration of the saline solution and inlet velocities corresponding to saline solution and sweeping air on the permeate flux on water production and thermal efficiency.

The inlet concentration has a small effect on the water production and the thermal efficiency of the SGMD device which presents an advantage of MD in comparison with usual techniques used for desalination such as reverse

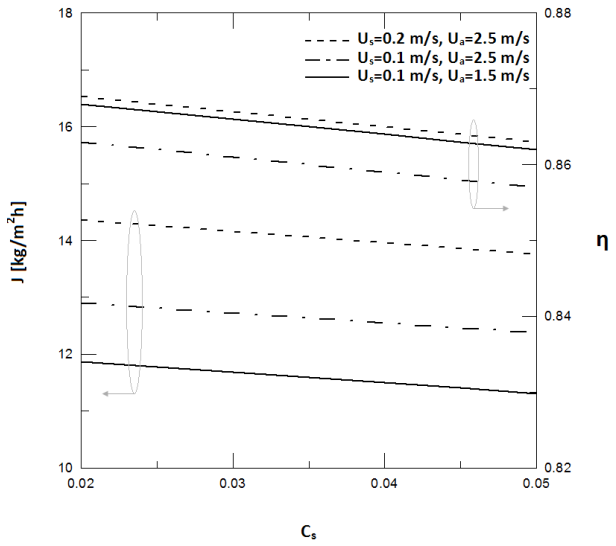

Fig. 9. Variation of permeate flux and thermal efficiency as a function of saline solution inlet concentration and inlet velocities.

osmosis. In fact, when C_s varies from 0.02 to 0.05, water production and thermal efficiency decrease by about 4% and 1% respectively.

5. Conclusions

This study presents a numerical investigation of a sweeping gas membrane distillation unit used for desalination. The governing equations expressing the conservation of mass, momentum, energy and species in the hot saline solution and the sweeping air were developed and solved numerically using the finite volume method. Numerical results were validated with experimental data. The results give a picture on the flow, heat and mass behavior in both domains of feed saline solution and weeping gas respectively. One of the main aims of the present study concerns the evaluation of the heat and mass transfer coefficients for such configurations. Obtaining accurate heat and mass transfer coefficients leads to contribute to improve the lumped models extensively used in MD theoretical analyses.

The main findings of this study can be summarized in the followings:

- simplified theoretical models such as the one developed by Khayet et al. [14] doesn't fit well the experimental data in comparison with the complete model presented in this study.
- pure water production and thermal efficiency are highly affected by inlet temperatures and slightly by inlet velocities of both flows (saline solution and sweeping air)
- varying saline solution inlet velocity U_s has no significant effect on the behavior of air heat transfer coefficient h_{xa} while h_{xs}, corresponding to the saline solution heat transfer, decreases with U_s decrease.
- increasing sweeping air inlet velocity tends to increase the heat transfer of the gas and to decrease the saline solution one.
- increasing membrane porosity or decreasing membrane material thermal conductivity enhances both water production and thermal efficiency.
- the inlet concentration of the saline solution has a small effect on the water production and the thermal efficiency even when varifying inlet velocities which presents an advantage of MD in comparison with usual techniques highly affected by salt concentration at the inlet.

Acknowledgments

The project was supported by King Saud University, Deanship of Scientific Research, College of Engineering Research Center.

Symbols

A — Membrane area [m²]
C — Mass fraction of NaCl
C_M — Mole fraction of NaCl
C_p — Specific heat [J kg^{-1} K^{-1}]
d — Half-width of the flow channel [m]
D_s — Diffusion coefficient of NaCl [m²/s]
$D_{v/a}$ — Coefficient of vapor-air mass diffusion [m²/s]
g — Acceleration of gravity [m/s²]
h_{fg} — Latent heat of evaporation [J/kg]
h_x — Local convective heat transfer coefficient [W/m²K]
J — Length-averaged permeate flux at the hot side of the membrane [kg/m²h]
J_v — Local permeate flux at the hot side of membrane, in vapor phase [kg/m²s]
K — Permeability of the membrane
k — Thermal conductivity [W/mK]
L — Membrane length [m]
m_a — Air flux [kg/s]
M_v — Molar mass of water vapor [kg k mol^{-1}]
N_x — Number of nodes along x direction
N_y — Number of nodes along y direction
P — Pressure [Pa]
Pr — Prandtl number
Q_C — Conductive heat flux [kJ/m²h]
Q_L — Latent heat flux [kJ/m²h]
Q_T — Total flux [kJ/m²h]
R — Universal gas constant [J/kmol K]
Re — Reynolds number
R_m — Thermal resistance of the membrane [m²K/W]
R_{mc} — Thermal resistance of the solid part of the membrane [m²K/W]
R_v — Thermal resistance of the vapor flow through membrane pores [m²K/W]
Sc — Schmidt number
T — temperature [°C]
U — Axial velocity component [m/s]
V — Radial velocity component [m/s]
w — Humidity ratio
w_a — Humidity at the membrane module inlet
x — Coordinate along to the solution flow [m]
y — Coordinate normal to the solution flow [m]
μ — Dynamic viscosity [kg m^{-1} s^{-1}]

υ — Cinematic viscosity [$m^2 s^{-1}$]
ρ — Density [kgm^{-3}]
ε — Porosity
χ — Tortuosity
δ — Membrane thickness [m]
η — Process thermal efficiency

Subscripts

a — Air
m — Membrane
ma — Membrane material
moy — Average
s — Saline solution
T — Total
v — Vapor

References

[1] N. Loussif, J. Orfi, Comparative study of air gap, direct contact and sweeping gas membrane distillation configurations, Membr. Water Treat., 7 (2016) 71–86.
[2] J. Orfi, N. Loussif, P.A. Davies, Heat and mass transfer in membrane distillation used for desalination with slip flow, Desalination, 381 (2016) 135–142.
[3] M.S. El-Bourawi, Z. Ding, R. Ma, M.A. Khayet, Framework for better understanding membrane distillation separation process, J. Membr. Sci., 285 (2006) 4–29.
[4] F. Anisi, K.M. Thomas, H.J. Kramer, Membrane-assisted crystallization: membrane characterization, modelling and experiments, Chem. Eng. Sci., 158 (2017) 277–286.
[5] L.M. Camacho, L. Dumée, J. Zhang, J. Li, M. Duke, J. Gomez, S. Gray, Advances in membrane distillation for water desalination and purification applications, Water, 5 (2013) 94–196.
[6] C.H. Lee, W.H. Hong, Effect of operating variables on the flux and selectivity in sweep gas membrane distillation for dilute aqueous isopropanol, J. Membr. Sci., 188 (2001) 79–86.
[7] Z. Xie, T. Duong, M. Hoang, C. Nguyen, B. Bolto, Ammonia removal by sweep gas membrane distillation, Water Res., 43 (2009) 1693–1699.
[8] M. Khayet, M.P. Godino, J.I. Mengual, Theoretical and experimental studies on desalination using the sweeping gas membrane distillation method, Desalination, 157 (2003) 297–305.
[9] L. Gao, J. Zhang, S. Gray, J.-D. Li, Experimental study of hollow fiber permeate gap membrane distillation and its performance comparison with DCMD and SGMD, Separ. Purif. Technol., 188 (2017) 11–23.
[10] S. Shuklaa, J.P. Méricqa, M.P. Bellevillea, N. Hengld, N.E. Benesb, I. Vankelecomc, J. Sanchez Marcanoa, Process intensification by coupling the Joule effect with pervaporation and sweeping gas membrane distillation, J. Membr. Sci., 545 (2018) 150–157.
[11] C. Cojocaru, M. Khayet, Sweeping gas membrane distillation of sucrose aqueous solutions: Response surface modeling and optimization, Separ. Purif. Technol., 81(1) 12–24.
[12] V. Karanikola, A.F. Corral, H. Jiang, A. Eduardo Sáez, W.P. Ela, Robert G. Arnold, Sweeping gas membrane distillation: Numerical simulation of mass and heat transfer in a hollow fiber membrane module, J. Membr. Sci., 483 (2015) 15–24.
[13] C.A. Rivier, M.C. García-Payo, I.W. Marison, U. von Stockar, Separation of binary mixtures by thermostatic sweeping gas membrane distillation I. Theory and simulations, J. Membr. Sci., 201 (2002) 1–16.
[14] M. Khayet, P. Godino, J.I. Mengual, Nature of flow on sweeping gas membrane distillation, J. Membr. Sci., 170 (2000) 243–255.
[15] M. Mahdi, A. Shirazi, A. Kargari, M. Tabatabaei, A.F. Ismail, T. Matsuura, Concentration of glycerol from dilute glycerol wastewater using sweeping gas membrane distillation, Chem. Eng. Proc., 78 (2014) 58–66.
[16] S. Shukla, N.E. Benes, I. Vankelecom, J.P. Méricq, M.P. Belleville, N. Hengl, J. Sanchez Marcano, Sweep gas membrane distillation in a membrane contactor with metallic hollow-fibers, J. Membr. Sci., 493 (2015) 167–178.
[17] M.C. Garcıa-Payo, C.A. Rivier, I.W. Marison, U. von Stockar, Separation of binary mixtures by thermostatic sweeping gas membrane distillation II. Experimental results with aqueous formic acid solutions, J. Membr. Sci., 198 (2002) 197–210.
[18] Z. Xie, T. Duong, M. Hoang, C. Nguyen, B. Bolto, Ammonia removal by sweep gas membrane distillation, Water Res., 43 (2009) 1693–1699.
[19] K. Charfi, M. Khayet, M.J. Safi, Numerical simulation and experimental studies on heat and mass transfer using sweeping gas membrane distillation, Desalination, 259 (2010) 84–96.
[20] S.-M. Huang, M. Yang, J. Tu, Y. Shao, Y. Zuo, Sweeping air membrane distillation: Conjugate heat and mass transfer in a hollow fiber membrane tube bank with an in-line arrangement, Int. J. Heat Mass Trans., 108 (2017) 2191–2197.
[21] A.M. Alklaibi, N. Lior, Transport analysis of airgap membrane distillation, J. Membr. Sci., 255 (2005) 239–253.
[22] K.W. Lawson, D.R. Lioyd, Membrane distillation, J. Membr. Sci., 124 (1997) 1–25.
[23] G.C. Sarti, C. Gostoli, S. Matulli, Low energy cost desalination processes using hydrophobic membranes, Desalination, 56 (1985) 277–286.
[24] A.M. Alklaibi, N. Lior, Heat and mass transfer resistance analysis of membrane distillation, J. Membr. Sci., 282 (2006) 362–369.
[25] M. Khayet, M.P. Godino, J.I. Mengual, Thermal boundary layers in sweeping gas membrane distillation processes, AIChE J., 48(7) (2002) 1488–1497.
[26] H.K. Versteeg, W. Malalasekera, (2007), An Introduction to Computational Fluid Dynamics: The Finite Volume Method, (2^{nd}ed.), Pearson and Prentice Hall,England.